

## REVIEW

## THE DIMENSIONALITY AND TOPOLOGY OF CHEMICAL BONDING MANIFOLDS IN METAL CLUSTERS AND RELATED COMPOUNDS

R. Bruce KING

*Department of Chemistry, University of Georgia, Athens, Georgia 30602, USA*

Received 22 January 1987

**Abstract**

The chemical bonding manifolds in metal cluster skeletons (as well as in skeletons of clusters of other elements such as boron or carbon) may be classified according to their dimensionalities and their chemical homeomorphism to various geometric structures. The skeletal bonding manifolds of discrete metal cluster polyhedra may be either one-dimensional edge-localized or three-dimensional globally delocalized, although two-dimensional face-localized skeletal bonding manifolds are possible in a few cases. Electron precise globally delocalized metal cluster polyhedra with  $\nu$  vertices have  $2\nu + 2$  skeletal electrons and form deltahedra with no tetrahedral chambers having total skeletal bonding manifolds chemically homeomorphic to a closed ball. Electron-rich metal cluster polyhedra with  $\nu$  vertices have more than  $2\nu + 2$  skeletal electrons and form polyhedra with one or more non-triangular faces, whereas electron-poor metal cluster polyhedra with  $\nu$  vertices have less than  $2\nu + 2$  skeletal electrons and form deltahedra with one or more tetrahedral chambers. Fusion of metal cluster octahedra by sharing (triangular) faces forms three-dimensional analogues of polycyclic aromatic hydrocarbons such as naphthalene, anthracene, and perinaphthenide. Fusion of metal cluster octahedra by sharing edges can be extended infinitely into one and two dimensions forming chains (e.g.  $\text{Gd}_2\text{Cl}_3$ ) and sheets (e.g.  $\text{ZrCl}$ ), respectively. Infinite extension of such fusion of metal cluster octahedra into all three dimensions leads to bulk metal structures. Unusual anionic platinum carbonyl clusters can be constructed from stacks of  $\text{Pt}_3$  triangles or  $\text{Pt}_5$  pentagons. The resulting platinum polyhedra appear to exhibit edge-localized bonding, supplemented by unusual types of delocalized bonding at the top and the bottom of the stacks. Superconducting ternary molybdenum chalcogenides and lanthanide rhodium borides consist of infinite lattices of electronically linked edge-localized  $\text{Mo}_6$  octahedra or  $\text{Rh}_4$  tetrahedra, leading naturally to the idea of porous delocalization in superconducting materials.

## 1. Introduction

In recent years, the chemistry of metal cluster compounds has attracted increasing interest [1]. Such compounds are constructed from polyhedra having metal atoms at the vertices. The structures of key types of metal cluster compounds have been established by X-ray crystallography.

A variety of theoretical approaches have been developed to treat chemical bonding in metal cluster compounds, as well as related cluster compounds having non-metals such as boron and carbon at the vertices. A key aspect in the early development of such theories is the recognition of the close relationships between polyhedral boranes and carboranes on the one hand, and transition metal clusters on the other hand [2]. Important theoretical approaches include our graph theory derived method [3–6], the original Wade–Mingos skeletal electron pair method [7–9], the extended Hückel calculations by Lauher [10], the perturbed spherical shell theory by Stone [11,12], and the topological electron counting method by Teo [13–16]. Strengths of our graph theory derived method include the following:

(1) The ability to deduce important information about the electron counts and shapes of diverse metal clusters using a minimum of computation.

(2) The ability to generate reasonable electron-precise bonding models for metal clusters that appear intractable by other methods not requiring heavy computation.

(3) Information concerning the distribution of total cluster electron counts between skeletal bonding within the cluster polyhedra and bonding to external ligands.

(4) Ability to distinguish between localized and delocalized bonding in cluster polyhedra.

This last point leads naturally to the concepts of the topologies and dimensionalities of metal cluster chemical bonding manifolds. Thus, the chemical bonding manifold of an edge-localized metal cluster is the 1-skeleton [17] of the underlying polyhedron and therefore is one-dimensional. However, the chemical bonding manifold of a globally delocalized metal cluster includes the whole volume of the underlying polyhedron and therefore is three-dimensional. Such concepts appear to be of practical as well as theoretical interest. For example, relatively high critical superconducting temperatures and magnetic fields in infinite metal cluster structures appear to be associated with a one-dimensional rather than a three-dimensional infinite chemical bonding manifold, leading naturally to the concept of porous delocalization [18,19].

This paper reviews some topological and dimensional ideas relative to understanding the structure and bonding in diverse types of metal clusters. In contrast to previous presentations of related ideas [3–6], this paper stresses the topological aspects of this theory and minimizes certain chemical details related to electron counting procedures and atomic orbital properties. This paper thus attempts to make some of the more interesting topological ideas in metal cluster structure and bonding

accessible to mathematicians as well as chemists. Readers wishing to supplement the topological ideas in this paper with chemical details are referred to the earlier presentations of this theory [3–6] and the further references cited therein.

## 2. Dimensionality and topology of chemical bonding

Consider a set of  $n$  atoms forming an  $n$ -center bond by overlap of appropriate atomic orbitals. The minimum number of dimensions  $d$  necessary to contain the  $n$  atoms can be called the *dimensionality* of the chemical bond. The dimensionality of the chemical bond can only be the integers 1, 2, or 3 and cannot exceed  $n - 1$ . If  $d = n - 1$ , then the chemical bond may be called *simplicial*. All two-center bonds must be simplicial and one-dimensional. In addition, all three-center bonds involving atoms in a triangle are simplicial and two-dimensional. The only examples of three-dimensional chemical bonds are derived from the  $n$ -center core bond in a globally delocalized polyhedron [3–6]; such bonds are almost never simplicial since  $n \geq 6$  in almost all cases.

Two topological spaces are homeomorphic if there are one-to-one mappings from one to the other that stretch and bend their domains into their ranges without tearing [20]. An analogous concept of *chemical homeomorphism* can be used to characterize the topologies of chemical bonding manifolds by relationships to familiar types of geometric structures. In this context, a triangular face of a polyhedron may be regarded as chemically homeomorphic to a closed surface, whereas a face with more than three edges may be regarded as chemically homeomorphic to an open hole. This is related to an idea apparently first presented by Kettle [21] in 1965. In this sense, a deltahedron having no tetrahedral chambers becomes chemically homeomorphic to a sphere and a polyhedron having one non-triangular face (and no tetrahedral chambers) becomes chemically homeomorphic to a sphere with a hole in it (i.e. a singly punctured sphere). More complicated polyhedral metal clusters can be chemically homeomorphic to more complicated surfaces or other geometric structures.

## 3. Elementary examples of different chemical bonding dimensionalities

### 3.1. ONE-DIMENSIONAL

The only type of one-dimensional chemical bond is the ubiquitous two-center bond between a pair of atoms characteristic of localized structures. Edge-localized polyhedral metal clusters may be regarded as chemically homeomorphic to the 1-skeleton [17] of the polyhedron. Such edge-localized polyhedral metal clusters are found when the vertex degrees of the polyhedron match the numbers of internal orbitals used by the vertex atoms [5,6]. Since vertex atoms normally use three internal orbitals, edge-localized polyhedra normally are those with degree 3 vertices such as

the tetrahedron, cube, prisms, and the regular  $I_h$  dodecahedron. Prototypical examples of edge-localized metal polyhedra are the tetrahedral metal cluster carbonyls  $M_4(CO)_{12}$  ( $M = Co, Rh, Ir$ ) and their derivatives. In some cases, early transition metal vertices use four rather than three internal orbitals. In such cases, edge-localized metal octahedra are possible [5,22]. Prototypical examples of edge-localized metal octahedra are found in molybdenum (II) halide derivatives of the type  $Mo_6Cl_8L_6^{4+}$ .

### 3.2. TWO-DIMENSIONAL

Examples of two-dimensional chemical bonds are found in planar polygons and in networks of triangles. The two-dimensional bonding in planar polygons (other than triangles) is non-simplicial. Examples of such systems include planar aromatic hydrocarbons such as cyclopentadienide, benzene, and tropylium, as well as analogous metal cluster systems such as  $Bi_4^{2-}$  and  $Se_4^{2+}$ . The total skeletal chemical bonding manifold of a planar polygon molecule such as benzene consists of a two-dimensional open manifold from the so-called  $\pi$ -bonding bounded by a one-dimensional circumference from the so-called  $\sigma$ -bonding. Such a total skeletal bonding manifold is chemically homeomorphic to a closed disk, in which the boundary is the one-dimensional bonding manifold and the interior is the two-dimensional bonding manifold. The two-dimensional bonding in networks of triangles is best exemplified by the surface bonding in a deltahedral metal cluster. Such a two-dimensional skeletal bonding manifold most commonly encloses a three-dimensional skeletal bonding manifold in globally delocalized deltahedral metal clusters. An exceptional example of an *empty* closed two-dimensional skeletal bonding manifold is found in the *face-localized* octahedral niobium clusters of the type  $Nb_6Cl_{12}L_6^{2+}$  (ref. [22]). Such a bonding manifold is chemically homeomorphic to an (empty) sphere and requires four rather than the normal three internal orbitals from each vertex atom [22]. Unusual examples of two-dimensional chemical bonding manifolds are found in the Möbius strips formed by sets of orbitals at each end of the stacked triangle platinum carbonyl anion clusters [23,24].

### 3.3. THREE-DIMENSIONAL

Three-dimensional chemical bonding corresponds to delocalization throughout a volume and is exemplified by the core bonding in globally delocalized deltahedral clusters [3–6]. The total skeletal bonding manifold of a globally delocalized deltahedral cluster consists of a three-dimensional open manifold from the core bonding bounded by a two-dimensional surface from the surface bonding. Such a bonding manifold is chemically homeomorphic to a closed ball, in which the boundary is the two-dimensional surface bonding manifold and the interior is the three-dimensional core bonding manifold.

Table 1

Relationships between vertex degree, bonding type, and chemical bonding manifold dimensionalities for the fundamental types of polygons and polyhedra<sup>a</sup>

Vertex degree	Cluster type	Bonding type	Skeletal bonding manifold dimensionalities
2	polygon	localized + delocalized	1 ("σ-bonding") 2 ("π-bonding")
3	"simple" polyhedron	localized	1 (i.e. 1-skeleton)
4	deltahedron (without tetrahedral chambers)	delocalized	2 (surface bonding) 3 (core bonding)

<sup>a</sup>These relationships apply for *normal* vertex atoms using three internal orbitals for skeletal bonding.

Table 2

The types of chemical bonding manifolds for discrete octahedral metal clusters

Bonding type	Internal orbitals from each vertex atom	Skeletal bonding manifold dimensionalities	Examples <sup>a</sup>
Edge-localized	4	1 (i.e. 1-skeleton)	$\text{Mo}_6\text{X}_8\text{L}_6^{4+}$ , " $\text{Mo}_6\text{Cl}_{12}$ ", Chevrel phases
Face-localized	4	2 (i.e. empty closed surface)	$\text{Nb}_6\text{X}_{12}\text{L}_6^{2+}$
Globally delocalized	3	2 (surface bonding) 3 (core bonding)	$\text{Zr}_6\text{Cl}_{12}\text{Be}$ , $\text{Zr}_6\text{Cl}_{13}\text{B}$ , $\text{Zr}_6\text{Cl}_{15}\text{N}$ , $\text{Rh}_6(\text{CO})_{16}$ , $\text{Os}_6(\text{CO})_{18}^-$

<sup>a</sup>L refers to electron pair donor ligands (including lone electron pairs from halogens or chalcogens bridging two other octahedra); the Be, B, and N atoms in the  $\text{Zr}_6$  clusters are located in the center of the  $\text{Zr}_6$  octahedra.

The relationships between different cluster types and the dimensionalities of their skeletal bonding manifolds are illustrated in tables 1 and 2. Table 1 summarizes relationships between the vertex degree, bonding type, and skeletal bonding manifold dimensionalities for the fundamental types of polygons and polyhedra. Table 2 summarizes the different types of skeletal bonding manifolds for discrete octahedral metal clusters.

#### 4. Maximally delocalized discrete metal cluster polyhedra

The discrete metal cluster polyhedra of interest are those with skeletal bonding manifolds which are maximally delocalized and hence of maximum dimensionality, namely 3. These are to be contrasted with the edge-localized and face-localized metal clusters discussed above having skeletal bonding manifolds of dimensionalities 1 and 2, respectively. Maximally delocalized metal cluster polyhedra are classified by the number of skeletal electrons relative to the number of vertices; details of the electron counting are presented elsewhere [3–6].

##### 4.1. ELECTRON PRECISE DELTAHEDRA ( $2v + 2$ SKELETAL ELECTRONS)

Such electron precise deltahedra have no tetrahedral chambers, i.e. no degree 3 vertices. The octahedron is the smallest deltahedron with these properties and is the fundamental building block for many metal cluster structures, including those with fused metal polyhedra [22]. The properties of such electron precise deltahedra having from six to twelve vertices are summarized in table 3.

Table 3  
Properties of some deltahedra without tetrahedral chambers<sup>a,b</sup>

Vertices	Deltahedron name <sup>a</sup>	Edges	Faces	Symmetry	Vertices of degrees		
					4	5	6
6	Octahedron	12	8	$O_h$	6	0	0
7	Pentagonal bipyramid	15	10	$D_{5h}$	5	2	0
8	Bisdisphenoid ("D <sub>2d</sub> dodecahedron")	18	12	$D_{2d}$	4	4	0
9	4, 4, 4-tricapped trigonal prism	21	14	$D_{3h}$	3	6	0
10	4, 4-bicapped square antiprism	24	16	$D_{4d}$	2	8	0
11	B <sub>11</sub> H <sub>11</sub> <sup>2-</sup> polyhedron	27	18	$C_{2v}$	2	8	1
12	Icosahedron	30	20	$I_h$	0	12	0

<sup>a</sup>For deltahedra having eight or more vertices, the deltahedron having the minimum number of degree 6 vertices (without introducing any degree 3 vertices) is chosen. For two such deltahedra, the deltahedron having maximum symmetry is chosen. The designations "4, 4, 4-tricapped" and "4, 4-bicapped" refer to capping square or rectangular faces in smaller polyhedra.

<sup>b</sup>Note that the number of vertices ( $v$ ), edges ( $e$ ), and faces ( $f$ ) of all of these polyhedra satisfy the Euler formula  $e + 2 = v + f$ .

The total skeletal bonding manifold of an electron precise deltahedron having  $v$  vertices consists of two parts, namely the surface and core bonding manifolds. The surface bonding manifold is a hybrid of chains of  $v$  pairs of two-center bonds corre-

sponding to the Hamiltonian circuits of the deltahedron. These two-center bonds use the tangential or twin internal orbitals of the vertex atoms. The hybridization process converts the one-dimensional manifolds of the chains corresponding to individual Hamiltonian circuits into two-dimensional manifolds chemically homeomorphic to the sphere. The core bonding manifold consists of a single  $v$ -center core bond formed by overlap of the radial or unique internal orbitals in the center of the deltahedron and is chemically homeomorphic to an open ball. The total skeletal bonding manifold of electron precise deltahedra is the sum of the surface and core bonding manifolds and is chemically homeomorphic to a closed ball in which the boundary is the surface bonding manifold and the interior is the core bonding manifold.

#### 4.2. ELECTRON-RICH POLYHEDRA (MORE THAN $2v + 2$ SKELETAL ELECTRONS)

Electron-rich polyhedra are polyhedra having one or more non-triangular faces. In boron hydride chemistry [25,26], such polyhedra have the special names nido, arachno, hypso, and klado, corresponding to  $2v + 4$ ,  $2v + 6$ ,  $2v + 8$ , and  $2v + 10$  skeletal electrons, respectively, for polyhedra having  $v$  vertices. An increase in the number of skeletal electrons relative to the number of vertices leads to an increase in the number and/or sizes of the non-triangular faces. The most important electron-rich polyhedra are the pyramids. These correspond to  $2v + 4$  skeletal electron nido systems, in which the base of the pyramid is the single non-triangular face.

The total skeletal bonding manifold of electron-rich polyhedra consists of three parts, namely the surface, hole, and core bonding manifolds. The two-dimensional surface bonding manifold is similar to that in the electron precise deltahedra discussed above except that it has holes corresponding to the non-triangular faces of the electron-rich polyhedron. The surface bonding manifold of electron-rich polyhedra is thus chemically homeomorphic to a sphere with holes in it, i.e. a *punctured sphere*. The hole bonding manifolds are two-dimensional, involve only orbitals of atoms bordering the holes, and are closely related to the two-dimensional bonding manifold of planar polygons (see above). The hole bonding manifolds thus function as patches for the holes in the surface bonding manifolds. The core bonding manifolds in electron-rich polyhedra are similar to those in electron precise deltahedra except that they now involve unique internal (radial) orbitals of only the interior vertex atoms, i.e. vertex atoms not bordering holes [3,5,6]. For this reason, an excessive number of non-triangular faces (i.e. topological holes) destroys the possibility for a delocalized skeletal bonding manifold.

The total skeletal bonding manifold of electron-rich polyhedra is chemically homeomorphic to a closed ball like the total skeletal bonding manifold of electron precise deltahedra. In both cases, the interiors of these manifolds consist of the core bonding manifolds, which are chemically homeomorphic to open balls. However, in the case of the electron-rich polyhedra, the boundary of the total skeletal bonding manifold is the sum of the surface and hole bonding manifolds, with the hole bonding

manifolds patching the holes in the surface bonding manifolds, leading to a boundary which is chemically homeomorphic to an unpunctured sphere.

#### 4.3. ELECTRON-POOR CAPPED DELTAHEDRA (LESS THAN $2v + 2$ SKELETAL ELECTRONS)

Electron-poor capped deltahedra are constructed from a *central deltahedron* without tetrahedral chambers by capping one or more of its triangular faces, thereby producing one tetrahedral chamber for each such cap. Alternatively, electron-poor polyhedra may be constructed by face-sharing fusion of one or more tetrahedra to the central deltahedron or to a smaller capped deltrahedron. A *decrease* in the number of electrons relative to the number of vertices (i.e. an increase in the "electron poverty") leads to an increase in the number of tetrahedral chambers. The best example of an electron-poor deltahedron is the capped octahedron in  $\text{Rh}_7(\text{CO})_{16}^{3-}$  (ref. [27]) or  $\text{Os}_7(\text{CO})_{21}$  (ref. [28]).

The total skeletal bonding manifold of such an electron-poor capped deltahedron consists of the sum of that of the central deltahedron and that of the tetrahedral chambers formed by the caps. The bonding in such tetrahedral chambers is edge-localized because the degree 3 vertex of the cap forming the chamber matches the three internal orbitals of the corresponding vertex atom. The chemical bonding manifold of the tetrahedral chamber is thus its 1-skeleton [17]. The total skeletal bonding manifold of a capped deltahedron with a globally delocalized central deltahedron consists of a closed ball corresponding to the central deltahedron with "tepee frames" on its surface corresponding to the 1-skeletons of the tetrahedral chambers.

This treatment of the chemical bonding topology of electron-poor capped deltahedra assumes that there is a central deltahedron without tetrahedral chambers. Such is *not* the case for the electron-poor  $\text{Os}_6(\text{CO})_{18}$ , which has a bicapped tetrahedron for its  $\text{Os}_6$  framework [28]. Such a bicapped tetrahedron can be constructed by fusing three tetrahedra through face sharing, just as a trigonal bipyramid can be constructed by an analogous fusion of two tetrahedra (fig. 1). Since the full volume of the  $\text{Os}_6$  framework in  $\text{Os}_6(\text{CO})_{18}$  consists of tetrahedral chambers, its total skeletal bonding manifold consists of the 1-skeleton of the bicapped tetrahedron corresponding to twelve two-center osmium-osmium bonds along the edges.

#### 4.4. POLYHEDRAL PUNCTURE AND POLYHEDRAL CAPPING

Consider an electron precise globally delocalized deltahedron having  $v$  vertices and the requisite  $2v + 2$  skeletal electrons. An electron-rich nido polyhedron with one non-triangular face,  $v - 1$  vertices, and  $2(v - 1) + 4 = 2v + 2$  apparent skeletal electrons can be formed by *polyhedral puncture*, i.e. making a hole in the deltahedral surface by removal of a vertex and all edges bonded to that vertex. Polyhedral puncture is a remedy for electron richness since it removes electrons but no bonding orbitals.



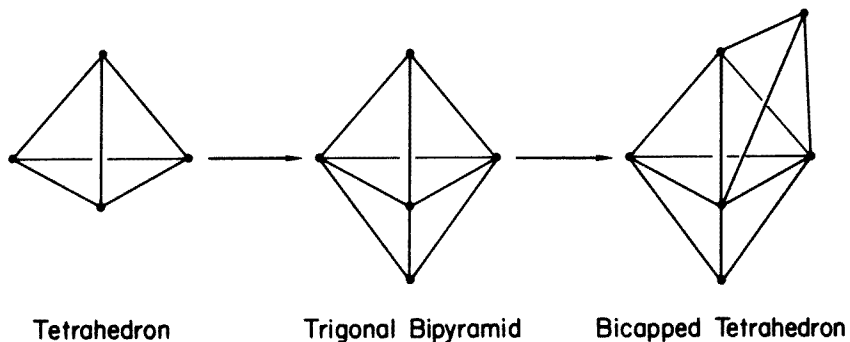


Fig. 1. Successive capping of a tetrahedron to give a trigonal bipyramid and bicapped tetrahedron (e.g. the  $\text{Os}_6$  framework in  $\text{Os}_6(\text{CO})_{18}$ ).

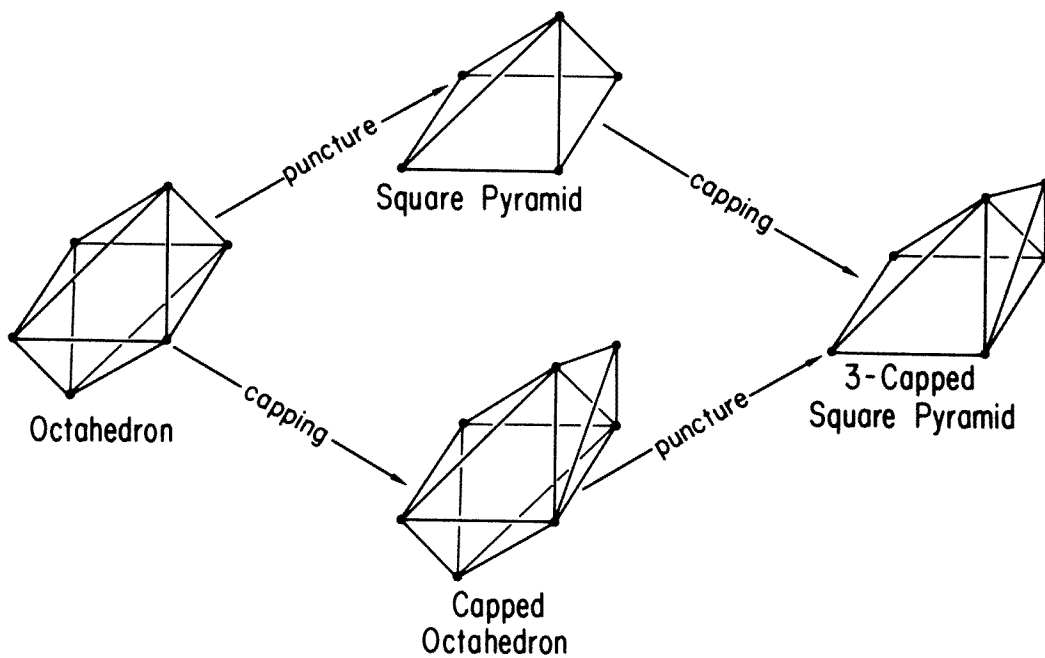


Fig. 2. Successive puncture and capping of an octahedron in either sequence to give the 3-capped square pyramid found in  $\text{H}_2\text{Os}_6(\text{CO})_{18}$ .

Conversely, an electron-poor capped deltahedron with one tetrahedral chamber,  $v + 1$  vertices, and  $2(v + 1) = 2v + 2$  apparent skeletal electrons can be formed by *polyhedral capping*, i.e. adding a vertex and three edges as a cap on one of the triangular faces of the deltahedron. Polyhedral capping is a remedy for electron poverty since it adds electrons but no bonding orbitals. Polyhedral puncture and polyhedral capping may be regarded as dual or complementary processes since they have opposite effects. An interesting example of a metal cluster formed from an electron precise deltahedron by successive application of polyhedral puncture and polyhedral capping in either order is  $\text{H}_2\text{Os}_6(\text{CO})_{18}$ . The  $\text{Os}_6$  framework in this cluster is a square pyramid with a capped triangular face [28]. This polyhedron can be formed from an octahedron by applying polyhedral puncture and polyhedral capping in either of the two possible sequences (fig. 2). The opposite effects of these dual processes on the electron count cancel each other so that the 3-capped square pyramidal  $\text{H}_2\text{Os}_6(\text{CO})_{18}$  has exactly the same 14 ( $= 2v + 2$  for  $v = 6$ ) skeletal electron count as the isoelectronic regular octahedral clusters  $\text{HOs}_6(\text{CO})_{18}^-$  and  $\text{Os}_6(\text{CO})_{18}^{2-}$  (ref. [28]).

## 5. Fused and linked metal cluster polyhedra

### 5.1. FUSION OF OCTAHEDRA

Polycyclic aromatic hydrocarbon structures are constructed from benzene rings by fusion of these hexagons so that they share edges. Thus, two-dimensional polygons fuse by sharing one-dimensional simplices [17] (i.e. edges). In an analogous way, metal cluster octahedra can fuse by sharing (triangular) faces to form more complicated metal cluster structures. In these cases, three-dimensional polyhedra fuse by sharing two-dimensional simplices [17] (i.e. triangular faces). Figure 3 summarizes these analogies using examples taken from the diverse areas of rhodium carbonyl anions [27] and molybdenum sulfides [18]. In the case of molybdenum sulfides, fusion of  $\text{Mo}_6$  octahedra by sharing faces can be extended infinitely, leading to linear  $[\text{Mo}_6\text{S}_6^{2-}]_\infty$  chains which are analogues of polyacenes.

Fusion of metal octahedra can also occur through edge sharing rather than face sharing. A finite example of such fusion is found in the ruthenium carbonyl carbide cluster anion  $\text{Ru}_{10}\text{C}_2(\text{CO})_{24}^{2-}$  (fig. 4, top). Infinite fusion of metal octahedra in this way is significant in providing a link between discrete metal clusters and bulk metal structures [22]. In the intermediate cases of such infinite fusion in one and two dimensions, the external surfaces of the metal cluster chains and sheets are protected by bridging halogen atoms. Such infinite fusion of  $\text{Gd}_6$  octahedra in one dimension leads to  $\text{Gd}_2\text{Cl}_3$  chains (fig. 4, bottom) containing two tetrahedral cavities for each octahedral cavity. The electron count in this system corresponds to globally delocalized bonding in both the octahedral and tetrahedral cavities, and therefore to a three-dimensional skeletal bonding manifold occupying the entire volume of the

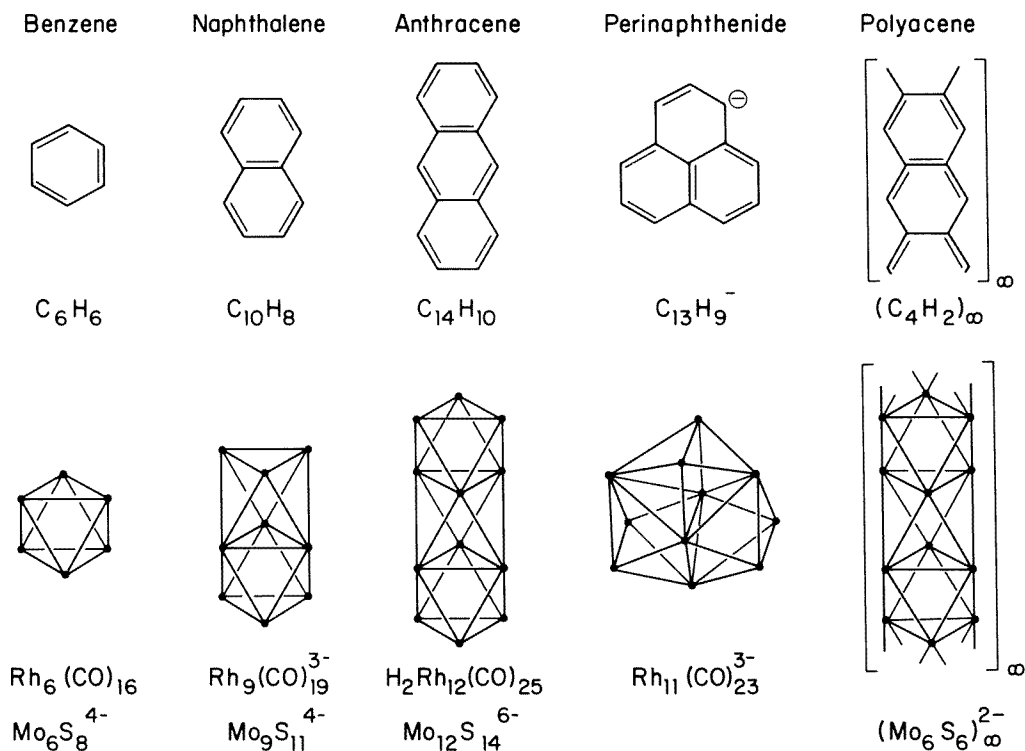


Fig. 3. Analogies between the fusion of metal octahedra in rhodium carbonyl and molybdenum sulfide clusters and the fusion of carbon hexagons (benzene rings) in planar polycyclic atomic hydrocarbons.

$Gd_2Cl_3$  chains. Such an interpretation leads to a closed shell electronic configuration for  $Gd_2Cl_3$  consistent with its semiconducting energy gap of approximately 1 eV [29]. Infinite fusion of metal octahedra in two dimensions leads to the sheet-like  $ZrCl$  structure similar to infinite fusion of benzene hexagons in two dimensions to give the sheet-like graphite structure [22]. The two-dimensional  $ZrCl$  structure, like the one-dimensional  $Gd_2Cl_3$  structure, has two tetrahedral cavities for each octahedral cavity, and an electron count corresponding to a single multicenter bond in each of the cavities [22].

Infinite fusion of metal octahedra in all three dimensions leads to bulk metal structures which frequently maintain the feature of two tetrahedral cavities for each octahedral cavity. Formation of a multicenter bond in each of these cavities leads to a total skeletal bonding manifold occupying the entire volume of space. This ultimate delocalization relates to the "electron gas" model for bulk metals [30] and accounts for their characteristic physical properties. Such multicenter bonding in the polyhedral cavities of a metal structure appears to be maximized for metals having six valence

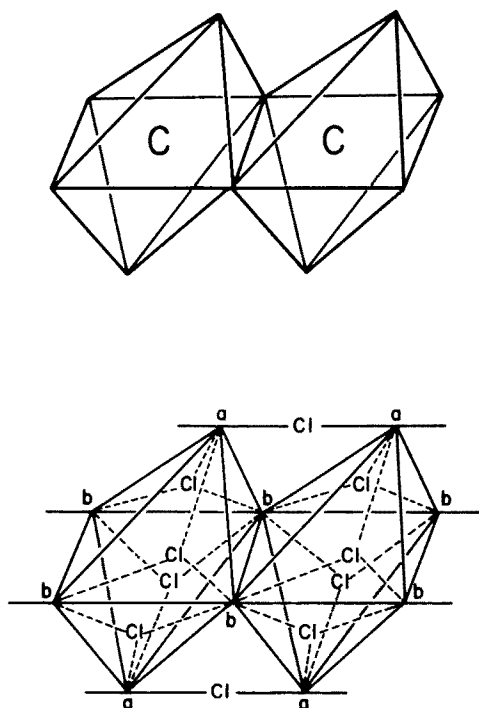


Fig. 4. (a) Top: The pair of carbon-centered edge-fused metal octahedra found in  $\text{Ru}_{10}\text{C}_2(\text{CO})_{24}^{2-}$ ; (b) Bottom: A unit of two octahedra found in the infinite chain  $\text{Gd}_2\text{Cl}_3$  structure based on edge-fused metal octahedra.

electrons [22] such as chromium, molybdenum, and tungsten, and correlates at least crudely with experimental information on the heats of atomization [31] and the properties of certain alloys [32].

## 5.2. ANIONIC PLATINUM CARBONYL CLUSTERS

Platinum forms some anionic carbonyl clusters exhibiting interesting structures [23,24]. The platinum frameworks of these clusters are illustrated in fig. 5. These structures may be constructed from stacks of platinum polygons having odd numbers of vertices. Rather unusual skeletal bonding topologies appear to be necessary to account for the electron counts and symmetries of these systems.

Consider first the stacked platinum triangle clusters of the general formula  $\text{Pt}_{3k}(\text{CO})_{6k}^{2-}$ , of which two examples are illustrated in fig. 5. The total skeletal bonding manifold consists of both one-dimensional and two-dimensional components. The one-dimensional component consists of the 1-skeleton of the triangle stack and corresponds to  $6k - 3$  edge-localized bonds for a  $\text{Pt}_{3k}(\text{CO})_{6k}^{2-}$  cluster. The two-dimen-

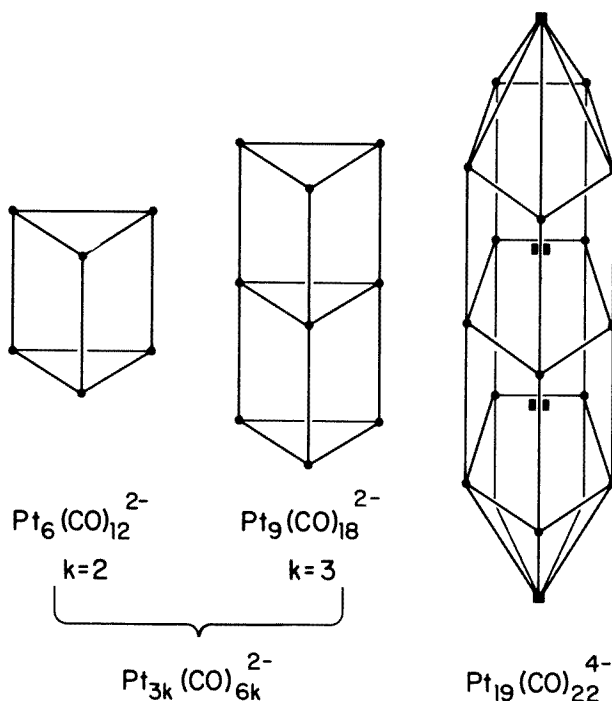


Fig. 5. Schematic diagrams of the stacked triangle platinum carbonyl anion clusters  $\text{Pt}_{3k}(\text{CO})_{6k}^{2-}$  ( $k = 2, 3$ ) and the threaded tubular stacked pentagon cluster  $\text{Pt}_{19}(\text{CO})_{22}^{4-}$ . In the  $\text{Pt}_{19}(\text{CO})_{22}^{4-}$  structure, the four platinum atoms of the  $\text{Pt}_4$  thread are shown as squares and the fifteen platinum atoms of the  $\text{Pt}_{15}$  stack of the three  $\text{Pt}_5$  pentagons are shown as circles. o

sional component consists of Möbius strips at both the top and bottom of the  $\text{Pt}_3$  triangles of the stack and is formed by metal  $d$  orbitals which undergo a phase change at each platinum atom of these triangles.

There is also one known platinum carbonyl structure based on stacked  $\text{Pt}_5$  pentagons, namely the  $\text{Pt}_{19}(\text{CO})_{22}^{4-}$  anion (fig. 5) [23,24]. The larger area of a pentagon relative to a triangle leads to the possibility of threading the tubular stack of three  $\text{Pt}_5$  pentagons with a thread of four platinum atoms so that there are pentagonal pyramid cavities at the top and bottom of the stack. The skeletal bonding manifolds in these pentagonal pyramid cavities are similar to those in isolated pentagonal pyramid structures, such as the borane  $\text{B}_5\text{H}_{10}$ , which are nido systems having 16 skeletal electrons ( $= 2v + 4$  for  $v = 6$ ). The total skeletal bonding manifold of  $\text{Pt}_{19}(\text{CO})_{22}^{4-}$  having the following components accounts for the electron count in this system:

- (a) One-dimensional: The 1-skeleton [17] of the  $\text{Pt}_{15}$  stack consisting of 25 edges as well as the three edges of the  $\text{Pt}_4$  thread;

- (b) Two-dimensional: The surfaces of the  $\text{Pt}_6$  pentagonal pyramids at each end of the  $\text{Pt}_{15}$  stack;
- (c) Three-dimensional: The cores of the  $\text{Pt}_6$  pentagonal pyramids at each end of the  $\text{Pt}_{15}$  stack.

### 5.3. POROUS DELOCALIZATION IN SUPERCONDUCTORS

Two classes of superconductors exhibiting relatively high critical temperatures and magnetic fields are the ternary molybdenum chalcogenides [18] and the ternary lanthanide rhodium borides [19]. Both of these classes of superconductors exhibit similar special features in their skeletal bonding topologies which can be described as *porous delocalization*. Such porously delocalized systems consist of lattices of linked *edge-localized* polyhedra in which the individual polyhedra are held close enough together and each polyhedron lacks one or two electrons of closed shell electronic configurations so that infinite electronic communication is possible in all three dimensions. In the case of the ternary molybdenum chalcogenides [18], the metal polyhedra are  $\text{Mo}_6$  octahedra, similar to those found in discrete octahedral molybdenum cluster halides (table 2). In the case of the ternary lanthanide borides [19], the metal polyhedra are  $\text{Rh}_4$  tetrahedra, similar to those found in the discrete rhodium cluster carbonyl  $\text{Rh}_4(\text{CO})_{12}$ . The skeletal bonding manifold of porously delocalized systems, although extending infinitely into all three dimensions, is only one-dimensional, consisting of the 1-skeletons of individual metal polyhedra linked by localized chemical bonds. From a physical point of view, this appears to relate to localization of the conduction electron wave function on the metal polyhedra, leading to an extremely short mean free path and/or a low Fermi velocity corresponding to a small B.C.S. coherence length [33].

The ternary molybdenum chalcogenides of interest are the Chevrel phases of general formulae  $\text{M}_n\text{Mo}_6\text{S}_8$  and  $\text{M}_n\text{Mo}_6\text{Se}_8$  ( $\text{M} = \text{Ba}, \text{Sn}, \text{Pb}, \text{Ag}, \text{lanthanides}, \text{Fe}, \text{Co}, \text{Ni}, \text{etc.}$ ). These phases were the first superconducting ternary systems found to have relatively high critical temperatures [34], reaching 15 K for  $\text{PbMo}_6\text{S}_8$ . In addition, the upper critical field of  $\text{PbMo}_6\text{S}_8$  ( $H_{c2} \approx 60$  T) is the highest value observed for any class of superconductors [35]. From the structural point of view, these Chevrel phases are constructed from  $\text{Mo}_6\text{S}_8$  (or  $\text{Mo}_6\text{Se}_8$ ) units containing a bonded  $\text{Mo}_6$  octahedron with a sulfur atom capping each face, leading to an  $\text{Mo}_6$  octahedron within an  $\text{S}_8$  cube. Each sulfur atom furnishes four electrons to the  $\text{Mo}_6$  octahedron within its  $\text{S}_8$  cube and its remaining two electrons to an adjacent  $\text{Mo}_6$  octahedron. Maximizing this latter bonding results in a tilting of the  $\text{Mo}_6$  octahedron by about  $25^\circ$  within the cubic array of the other metal atoms  $\text{M}$  (e.g.  $\text{Pb}$  in  $\text{PbMo}_6\text{S}_8$ ) [36]. These other metal atoms  $\text{M}$  furnish electrons to the  $\text{Mo}_6\text{S}_8$  units, allowing them to approach but not attain the  $\text{Mo}_6\text{S}_8^{4-}$  closed shell electronic configuration. This corresponds to a partially filled valence band. Electronic bridges between individual  $\text{Mo}_6$  octahedra are provided by interoctahedral metal-metal interactions. Thus, for  $\text{Mo}_6\text{S}_8$

derivatives, the nearest *interoctahedral* Mo-Mo distances fall in the range 3.08 to 3.49 Å as contrasted with the *intraoctahedral* Mo-Mo distances in the range 2.67 to 2.78 Å.

The ternary lanthanide rhodium borides have the general formulae  $\text{LnRh}_4\text{B}_4$  (Ln = certain lanthanides such as Nd, Sm, Er, Tm, Lu) and exhibit significantly higher superconducting transition temperatures than other types of metal borides [19]. Their structures consist of  $\text{Rh}_4\text{B}_4$  units containing a bonded  $\text{Rh}_4$  tetrahedron with a boron atom capping each face, leading to an  $\text{Rh}_4\text{B}_4$  cube with 2.17 Å Rh-B bonds along each of the twelve edges and 2.71 Å Rh-Rh bonds along six face diagonals. The ratio between these two bond lengths, namely  $2.71/2.17 = 1.25$ , is only about 13% less than the  $\sqrt{2} = 1.414$  ratio of these lengths in an ideal cube. The lanthanides, Ln, furnish three electrons to the  $\text{Rh}_4\text{B}_4$  cube, allowing them to approach, but still fall one electron short of the closed shell electronic configuration  $\text{Rh}_4\text{B}_4^{4-}$ . Again, this corresponds to a partially filled valence band. The  $\text{Rh}_4\text{B}_4$  cubes are held close enough for electronic communication between adjacent cubes by means of inter-cube B-B and Rh-Rh bonding.

## 6. Summary

This paper shows how topological and dimensional ideas are useful for characterizing the skeletal chemical bonding in the diverse variety of metal cluster structures. Of particular importance in polyhedral metal clusters is the contrast between one-dimensional edge-localized skeletal bonding and three-dimensional globally delocalized skeletal bonding. One-dimensional edge-localized skeletal bonding appears to be preferred when the vertex degrees match the numbers of internal orbitals from the corresponding vertex atoms.

Methods for fusing and linking metal cluster polyhedra are also of interest. Metal octahedra can be fused by sharing either faces or edges. Metal clusters constructed from the face sharing of metal octahedra may be regarded as three-dimensional analogues of polycyclic aromatic systems constructed from the edge sharing of carbon hexagons. Edge sharing of metal octahedra can be extended indefinitely into one and two dimensions, leading to  $\text{Gd}_2\text{Cl}_3$  chains and  $\text{ZrCl}$  sheets, respectively. The limiting case of infinite edge sharing of metal octahedra in all three dimensions corresponds to the bulk metal structures.

Special cases of fused metal polyhedral clusters are found in anionic platinum carbonyl clusters, which are constructed by stacking  $\text{Pt}_3$  triangles or  $\text{Pt}_5$  pentagons. The  $(\text{Pt}_5)_k$  pentagonal stack is threaded by an additional  $\text{Pt}_{k+1}$  chain ( $k = 3$ ). The resulting polyhedra appear to exhibit edge-localized bonding supplemented by unusual types of delocalization at both the top and the bottom of the stacks.

These topological and dimensional ideas appear to be important for understanding the physical properties of materials based on metal cluster structures. Thus,

the superconducting ternary molybdenum chalcogenides and ternary lanthanide rhodium borides exhibiting relatively high superconducting transition temperatures and/or magnetic fields appear to consist of infinite lattices of electronically linked edge-localized metal polyhedra (i.e. Mo<sub>6</sub> octahedra or Rh<sub>4</sub> tetrahedra), leading naturally to the idea of porous delocalization in superconducting materials. This observation suggests that a more detailed understanding of metal cluster bonding topologies will provide a basis for the design of novel solid-state materials with interesting and useful electrical, magnetic, and optical properties including superconductors, semiconductors, photoconductors, ferromagnets, and laser materials.

## Acknowledgements

The author is indebted to the U.S. Office of Naval Research for partial support of this work. The ideas outlined in this paper were presented initially at the 1985 Spring Topology Conference held at the Florida State University, Tallahassee, Florida, U.S.A., March 1985.

## References

- [1] B.F.G. Johnson, ed., *Transition Metal Clusters* (Wiley-Interscience, Chichester, England, 1980).
- [2] K. Wade, *Chem. Commun.* (1971) 792.
- [3] R.B. King and D.H. Rouvray, *J. Amer. Chem. Soc.* 99(1977)7834.
- [4] R.B. King, *Inorg. Chim. Acta* 57(1982)79.
- [5] R.B. King, in: *Chemical Applications of Topology and Graph Theory*, ed. R.B. King (Elsevier, Amsterdam, 1983) pp. 99 – 123.
- [6] R.B. King, in: *Molecular Structure and Energetics*, ed. J.F. Liebman and A. Greenberg (VCH, Deerfield Beach, Florida, 1986) pp. 123 – 148.
- [7] D.M.P. Mingos, *Nature (London) Phys. Sci.* 236(1972)99.
- [8] K. Wade, *Adv. Inorg. Chem. Radiochem.* 18(1976)1.
- [9] D.M.P. Mingos, *Accts. Chem. Res.* 17(1984)311.
- [10] J.W. Lauher, *J. Amer. Chem. Soc.* 100(1978)5305.
- [11] A.J. Stone, *Inorg. Chem.* 20(1981)563.
- [12] A.J. Stone, *Polyhedron* 3(1984)1299.
- [13] B.K. Teo, *Inorg. Chem.* 23(1984)1251.
- [14] B.K. Teo, G. Longoni and F.R.K. Chung, *Inorg. Chem.* 23(1984)1257.
- [15] B.K. Teo, *Inorg. Chem.* 24(1985)115.
- [16] B.K. Teo, *Inorg. Chem.* 24(1985)4209.
- [17] B. Grünbaum, *Convex Polytopes* (Interscience, New York, 1967).
- [18] R.B. King, *J. Solid State Chem.*, in press.
- [19] R.B. King, *J. Solid State Chem.*, in press.
- [20] M.J. Mansfield, *Introduction to Topology* (Van Nostrand, Princeton, 1963).
- [21] S.F.A. Kettle, *Theor. Chim. Acta* 3(1965)282.



- [22] R.B. King, *Inorg. Chim. Acta* 129(1987)91.
- [23] R.B. King, in: *Mathematics and Computational Concepts in Chemistry*, ed. N. Trinajstić (Harwood, Chichester, 1986) pp. 146 – 154.
- [24] R.B. King, *Inorg. Chim. Acta* 116(1986)119.
- [25] R.W. Rudolph and W.R. Pretzer, *Inorg. Chem.* 11(1972)1974.
- [26] R.W. Rudolph, *Accts. Chem. Res.* 9(1976)446.
- [27] R.B. King, *Int. J. Quant. Chem.* 20S(1986)227.
- [28] R.B. King, *Inorg. Chim. Acta* 116(1986)99.
- [29] D.W. Bullett, *Inorg. Chem.* 24(1985)3319.
- [30] C. Kittel, *Introduction to Solid State Physics*, Third Edition (Wiley, New York, 1966) Chs. 7 and 8.
- [31] W.E. Dasent, *Inorganic Energetics* (Penguin Books, Ltd., Baltimore, 1970).
- [32] H.E.N. Stone, *Acta Metallurgica* 27(1979)259.
- [33] Ø. Fischer, M. Decroux, R. Chevrel and M. Sergent, in: *Superconductivity in d- and f-Band Metals*, ed. D.H. Douglas (Plenum Press, New York, 1976) pp. 176 – 177.
- [34] B.T. Matthias, M. Marezio, E. Corenzwit, A.S. Cooper and H.E. Barz, *Science* 175(1972) 1465.
- [35] S. Foner, E.J. McNiff, Jr. and E.J. Alexander, *Phys. Lett.* A49(1974)269.
- [36] J.K. Burdett and J.-H. Lin, *Inorg. Chem.* 21(1982)5.